

# Enhanced Protein Adsorption in Fibrous Substrates Treated with Zeolitic Imidazolate Framework-8 (ZIF-8) Nanoparticles

Hao Fu,<sup>+,†</sup> Pengfei Ou,<sup>+,‡</sup> Jia Zhu,<sup>§</sup> Pengfei Song,<sup>\*,||</sup> Jiquan Yang,<sup>\*,⊥</sup> and Ye Wu<sup>\*,⊥</sup>

<sup>†</sup>Department of Mechanical Engineering, McGill University, Montreal, Quebec H3A 0C3, Canada

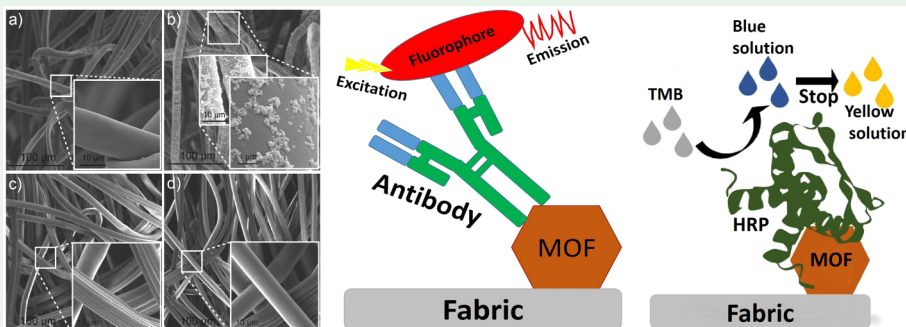
<sup>‡</sup>Department of Mining and Materials Engineering, McGill University, Montreal, Quebec H3A 0C5, Canada

<sup>§</sup>Wenzheng College, Soochow University, Suzhou 215104, China

<sup>||</sup>Department of Electrical and Electronic Engineering, Xi'an Jiaotong-Liverpool University, Suzhou, Jiangsu 215123, China

<sup>⊥</sup>School of Electrical and Automation Engineering, Jiangsu Key Laboratory of 3D Printing Equipment and Manufacturing, Nanjing Normal University, Nanjing, 210046, China

## Supporting Information



**ABSTRACT:** Development for new solid substrates for protein adsorption is important, given the massive potential in a number of fields including food production, medicine, biotechnology, and pharmaceutical processing. We developed a zeolitic imidazolate framework 8 (ZIF-8)-nanoparticles based fibrous platform (**Platform 1**). Its ability in protein adsorption is proven by fluorescence study of Alexa Fluor 647-labeled donkey anti-rabbit IgG adsorbed on **Platform 1**. Studies reveal that **Platform 1** shows much more enhanced protein adsorption compared to a polyethylene terephthalate gauze fibrous platform treated with ZIF-8 nanoparticles. This may be explained by considering that more active sites are enabled on fabric to adsorb a higher amount of ZIF-8 nanoparticles. We show that **Platform 1** provides favorable biocompatibility to maintain the bioactivity of enzymes. Furthermore, we prove that a carboxymethylated cotton fabric platform treated with ZIF-8 (**Platform 3**) can be more capable of immobilizing the Alexa Fluor 647-labeled antibodies than **Platform 1**. Carboxymethylation helps to enhance protein adsorption in these cotton fabric substrates.

**KEYWORDS:** protein adsorption, biocompatibility, carboxymethylation, substrates, MOFs

## 1. INTRODUCTION

Protein adsorption at solid surfaces exhibits an important role in widespread research areas including food processing, medicine, biotechnology, and pharmaceutical sciences.<sup>1,2</sup> The feasibility of protein adsorption on various substrates may yet be manifested in various problems when it is encountered in practical applications, such as unsatisfying biocompatibility,<sup>3</sup> complicated operations,<sup>4</sup> and huge cost.<sup>5</sup>

A good choice of a proper substrate with robust mechanical stability and cost-effectiveness is promising for harnessing the aforementioned issues. Fabrics, consisting of either natural or artificial fibers with three-dimensional porous structures, may be appropriate candidates as matrix substrates for protein adsorption.<sup>6</sup> Fabric fibers have been investigated as porous matrices for immobilizing proteins.<sup>7–10</sup> Indeed, the proteins (e.g., antibodies and enzymes) can be physically adsorbed on

the fabric fiber surface via van der Waals forces and electrostatic interactions.<sup>6,11</sup> Additionally, fabric fibers provide a potentially biocompatible environment for the proteins by retaining the maximal activity during the immobilization process.<sup>12</sup> Although physical adsorption is a main approach to immobilize proteins onto the fabric surface, the proteins are not strongly attached to the fabric fibers.<sup>6</sup> One common issue is that the proteins can be easily washed off or desorbed during assaying due to the weak interaction of physical adsorption.<sup>13</sup> Therefore, a more aggressive immobilization strategy for the proteins on the fabric surface is more likely to be required.

**Received:** September 6, 2019

**Accepted:** December 2, 2019

**Published:** December 2, 2019

In the emerging biochemical field, such as bacteria restraint, the employment of metal–organic frameworks (MOFs),<sup>14–16</sup> or the combination of MOFs and fabric fibers,<sup>17,18</sup> has attracted much attention.

These works enable widely used opportunities of MOF/fabric platforms in various fields. In the scenario of the MOFs/fabric platforms, the use of physical entanglement and van der Waals interactions between MOF nanocrystals and fabric surface is a primary way to achieve the attachments of MOFs.<sup>19</sup>

Adsorption effectiveness of MOFs is ulteriorly enhanced through metal ions in MOFs which can form electrostatic attractions with electronegative groups.<sup>20</sup> Thus, fabric fibers with electronegative surfaces (i.e., rich oxygen-containing functional groups) can be used to simply form robust coordination interactions with metal ions on MOFs.<sup>21,22</sup>

Taking advantage of several unique features, such as tunable pore size, pore shape, and pore volume based on alterable synthesis protocols, MOFs can create specific and strong interactions between MOFs and the proteins via surface adsorption,<sup>15</sup> covalent binding,<sup>23</sup> cage inclusion,<sup>24</sup> or in situ synthesis.<sup>25</sup> Therefore, by combining the characteristics of MOFs with superior attachments to fabric fibers and adsorptions for the proteins, MOFs are promising candidates as certain intermediates to improve protein immobilization on fabric matrices. However, as far as the authors know, there are no reports on MOF nanocrystals combined with fabric fiber surfaces as active binding sites for protein immobilization.

Zeolitic imidazolate frameworks (ZIFs) are examples of MOF crystals mostly fabricated by copolymerization of Zn (II) with imidazolate (IM)-type links.<sup>26</sup> Unlike other types of MOFs, ZIFs exhibit extraordinary stability in chemistry-related atmospheres,<sup>26</sup> exceptional thermal stability, and low cytotoxicity.<sup>27</sup> Benefiting from the chemical stability and flexibility, the ZIFs show promising potential as robust precursors to enable a substrate feasible for chemical or biological applications. As one of the ZIFs, ZIF-8 can be synthesized as a SOD-zeolite-net crystalline material with 2-methylimidazolate (MeIM)-unit structure. Compared to other Zn(IM)<sub>2</sub>-type ZIFs, the ZIF-8 has a large sphere up to a diameter of 11.6 Å.<sup>27</sup> It has a higher capability to fit in the cavity without touching the van der Waals atoms of the framework,<sup>28</sup> especially for biomolecules (e.g., proteins, nucleic acids). Interestingly, fabric fibers can improve the crystallization of ZIF-8 coatings around the fibers without any need for surface functionalization in a mild aqueous condition.<sup>29</sup> Therefore, a low-cost and feasible manufacturing process that can associate ZIF-8 nanocrystals with fabric substrates becomes possible.

It should be mentioned that the ZIF-8 has been used in a MOFs/fabric composite for gas adsorption.<sup>30</sup> Considering the chelation of zinc between hydroxy groups in fabric<sup>30,31</sup> and histidine residues in proteins,<sup>32</sup> ZIF-8 nanocrystals on a fabric fiber surface can be employed as grafted binding sites to enhance the capability of fabrics for protein adsorption.

Considering the abundance of hydroxyl groups existing in fabrics, chemical modifications of fabrics into functional groups (e.g., carboxymethyl groups) are feasible for enhancing target immobilization.<sup>33,34</sup> Also, fabric substrates have been demonstrated in maintaining its initial morphological integrity after introducing various chemically functional groups.<sup>34</sup> The metal ions in MOFs can be anchored to the functional groups on the modified fabric substrate after a carboxymethylation process.<sup>35</sup> Hence, the carboxymethylated cellulose enables more active sites on fabric to adsorb the MOF nanocrystals leading to a

high loading of MOF by not only chelation but also another type of electrostatic-like interaction.<sup>31</sup>

Herein, we report the development of a ZIF-8 nanoparticle-based fibrous platform, a cotton fabric platform treated with the ZIF-8 (**Platform 1**). Its ability for protein adsorption is examined via fluorescence study of Alexa Fluor 647-labeled donkey anti-rabbit IgG adsorbed on **Platform 1**. For comparison, a polyethylene terephthalate gauze fabric platform treated with the ZIF-8 nanoparticles (**Platform 2**) was also made. The results demonstrate that protein adsorption in **Platform 1** is significantly higher comparing to **Platform 2**. Moreover, we found out that a carboxymethylated cotton fabric platform treated with the ZIF-8 (**Platform 3**) performed with a more robust ability to immobilize the Alexa Fluor 647-labeled antibodies than **Platform 1** due to the carboxymethylated modification.

## 2. EXPERIMENTAL SECTION

**2.1. Materials.** Horseradish peroxidase (HRP) and 3,3',5,5'-Tetramethylbenzidine (TMB) were purchased from Bio-Rad (Hercules, CA). Methanol, dimethyl sulfoxide (DMSO), phosphate buffered saline (PBS), hydrogen peroxide, sulfuric acid, zinc nitrate hexahydrate, sodium chloroacetate, sodium hydroxide, and 2-methylimidazole were purchased from Sigma-Aldrich (St. Louis, MO). Alexa Fluor 647-labeled donkey anti-rabbit IgG (ab150075) was obtained from Abcam (Cambridge, MA). All the reagents were of analytical grade and used without further purification. Cotton gauze fabric and polyethylene terephthalate gauze from Johnson & Johnson were bought at local Rite Aid store (Baton Rouge, LA).

**2.2. Instrumentation.** A JEM-1011 (JEOL Ltd., Japan) transmission electron microscope (TEM) was used to image as-synthesized ZIF-8 nanocrystals at an acceleration voltage of 120 kV. Scanning electron microscopy (SEM) images were used to characterize the morphology of different fabrics utilizing a FEI Quanta-200 (Thermo Fisher Scientific, USA) environment scanning electronic microscope with a beam accelerating voltage of 5 kV. Before using SEM, all fabric samples were coated with 99.99% gold by an ion benchtop sputter coater (EMS Sciences).

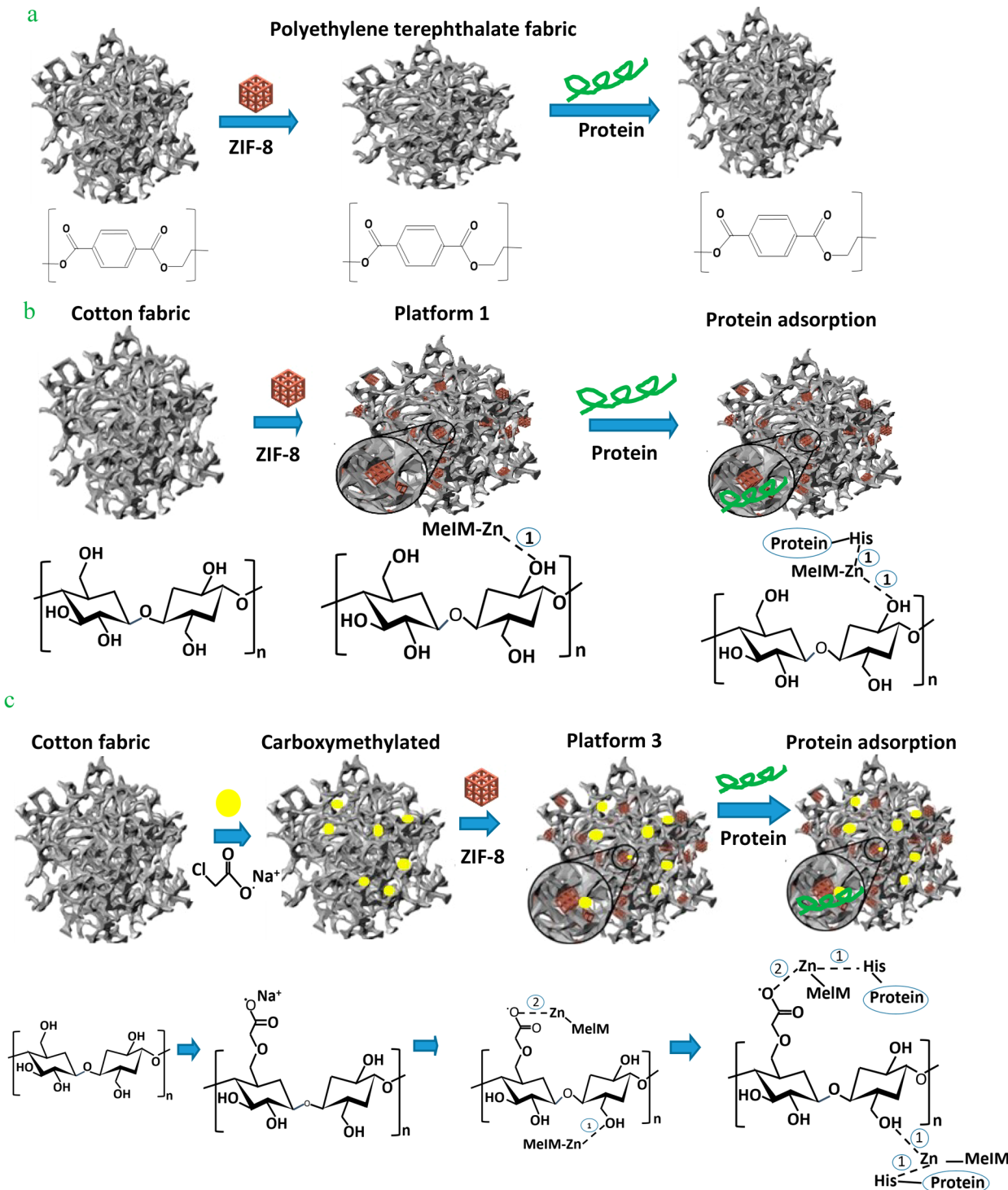
Powder X-ray diffraction (XRD) patterns were collected by a PANalytical Empyrean X-ray diffractometer (Malvern Panalytical Technology, USA) using Cu K $\alpha$  radiation of 40 kV and electric current 15 mA with a scan speed of 0.2° min<sup>-1</sup>, a step size of 0.005°, and a 2θ range of 5–40°.

X-ray photoelectron spectroscopy (XPS) analyses were done via a K $\alpha$  XPS instrument (Kratos AXIS 165, Kratos Analytical, USA). Three spots were positioned and analyzed for each sample with a spot size of 200 μm at a 50 eV pass energy from an incident monochromatic X-ray beam. Fourier transform infrared (FTIR) spectra were recorded with a Nicolet IS 10 FTIR spectrometer (Thermo Fisher Scientific Inc., Waltham, MA) in single attenuated total reflectance (ATR) mode. The spectra were collected in the range of 400–4000 cm<sup>-1</sup> at a resolution of 4 cm<sup>-1</sup> for 32 scans.

**2.3. Synthesis of ZIF-8 Nanoparticles.** To synthesize ZIF-8 nanoparticles, zinc nitrate hexahydrate (0.35 g) was resolved in 10 mL of deionized (DI) water. Then, 2-methylimidazole (6.65 g) was mixed in the solution under vigorous stirring. All the operations were done at room temperature. The solution turned milky instantly when the 2-methylimidazole was added. After stirring for ~80 min, the solution was centrifuged at 6000 rpm for 30 min, then 10 000 rpm for 30 min, and finally 14 000 rpm for 30 min to get the ZIF-8 nanoparticles.

**2.4. Preparation of Fabric Platform Treated with ZIF-8 Nanoparticles (**Platform 1**).** To prepare noncarboxymethylated fabric combined with ZIF-8 (**Platform 1**), the ZIF-8 nanocrystal solution (1.0 g) was resolved and suspended in 10 mL of DI water. Followed by placing a piece of cotton gauze fabric (0.1 g) into a glass Petri dish, the ZIF-8 nanocrystal solution was added into the Petri dish. The mixture was stirred vigorously at 60 °C for 2 h. Then, it was subsequently washed in deionized water and methanol each twice to

**Scheme 1.** (a) Polyethylene Terephthalate Fabric Fails To Attach ZIF-8 Nanoparticles and Cannot Perform Protein Adsorption. (b) Cotton Fabric Platform Treated with ZIF-8 Nanoparticles Can Be Used to Perform Protein Adsorption. (c) Carboxymethylation Process of Cotton Fabric, Adsorption of ZIF-8 on Platform 3, and Protein Adsorption<sup>a</sup>



<sup>a</sup>Dash line 1 represents chelation, and 2 represents electrostatic-like interaction.

remove residual MOF nanocrystals that were not attached to the fiber surface.

**2.5. Preparation of Polyethylene Terephthalate Gauze Platform Treated with ZIF-8 (Platform 2).** We also prepared a polyethylene terephthalate gauze based fibrous platform as reference for our study. Its preparation procedure was the same as that of Platform 1 by using the polyethylene terephthalate gauze rather than the cotton gauze fabric.

**2.6. Carboxymethylation of the Fabric Fibers.** In order to produce a fabric substrate with greater MOF attachment capability for higher yield of protein immobilization, cotton gauze fabric was chemically functionalized by a carboxymethylation method.<sup>35</sup> We used a piece of cotton gauze fabric to start the carboxymethylation of the fabric fibers.

The cotton gauze fabric (0.1 g) was immersed in 10 mL of a solution including 1 M sodium chloroacetate and 5% sodium

hydroxide, and the reaction was carried out under stirring for 1 h at room temperature. After the reaction, the carboxymethylated cotton gauze fabric was washed with deionized water to remove the residual reagents, and then was dried at room temperature overnight.

**2.7. Preparation of Carboxymethylated Fabric Platform Treated with ZIF-8 (Platform 3).** The carboxymethylated fabric treated with ZIF-8 (**Platform 3**) was prepared as follows. First, the as-synthesized ZIF-8 nanocrystal solution (1.0 g) was resolved and suspended in 10 mL of deionized water. Then, a piece of carboxymethylated cotton gauze fabric (0.1 g) was added in the ZIF-8 nanocrystal solution and the reaction was under stirring at 60 °C for 2 h. After the reaction, it was washed subsequently in DI water and methanol each twice and stored at room temperature overnight before characterization and biological assays.

**2.8. Protein Adsorption and Enzyme Biocompatibility of MOF/Fabric Platforms.** Fluorometric assays of protein adsorption on fabric were quantified using a fluorescent microscope (Olympus America Inc., Center Valley, PA) equipped with a camera (Amscope, Irvine, CA). The samples were immersed in 100 µg/mL Alexa Fluor 647-labeled donkey anti-rabbit IgG for 30 min, respectively. Then, they were transferred individually into a washing buffer (0.05% v/v Tween-20 in PBS) to be immersed for another 30 min to wash off unbound IgG. A small piece of fabric fibers was peeled off from the samples and adhered to a clean glass slide. The fabric fibers were observed by a fluorescence microscope (excitation and emission were set to 575 and 645 nm, respectively). The camera was used to capture images of fluorescent protein labeled fabrics and the fluorometric results were measured by ImageJ (NIH, Bethesda, MD).

A biocompatibility evaluation was carried out by measuring the enzyme adsorption performance and activity on **Platform 1** and **Platform 2**. To prepare the chromogenic substrate solution, HRP enzymes (200 µL of 1 mg/mL) were dissolved in 10 mL of PBS buffer. Then, TMB substrate (5 mg) was dissolved in 1 mL of DMSO, and then the chromogenic substrate solution was added to 9 mL of 0.05 M phosphate-citrate buffer (pH 5.0). Hydrogen peroxide (2 µL of fresh 30%) was added to 10 mL of substrate solution immediately prior to use. **Platform 1** and **Platform 2** were immersed in 20 µg/mL HRP solution first for 30 min, followed by washing in PBS buffer three times for 1 min each to remove the residual HRP enzymes on fabric fiber surfaces due to weak physical adsorption. Then, the samples were immersed in 500 µg/mL TMB substrate solution for another 30 min. Finally, a stop solution (10 mL of 2 M sulfuric acid) was added for coloration. The images of the composites were captured by an Epson V 550 desktop scanner (Epson America, Inc., Long Beach, CA) and quantified by ImageJ (NIH, Bethesda, MD).

### 3. RESULTS AND DISCUSSION

It should be noted that we used a polyethylene terephthalate gauze platform combined with the ZIF-8 (**Platform 2**) as a reference material for our study. The reason we used a polyethylene terephthalate matrix is because it is a fibrous matrix with a three-dimensional porous structure that has similar physical morphology to cotton fabric fiber.<sup>36</sup>

As shown in **Scheme 1**, cotton gauze fabric platforms with hydroxy groups are supposed to have a higher possibility to immobilize MOF nanocrystals than the polyethylene terephthalate matrix with carbonyl groups.<sup>31,37</sup>

We intended to verify that the three-dimensional porous matrices in textile cotton fabric with proper functional groups can contribute to the MOF adsorptions and further protein immobilizations, which is not only dependent on the physical morphology.

**3.1. XRD, TEM, and SEM Analyses.** By comparing the powder XRD pattern of our ZIF-8 nanocrystals with reported works<sup>26,38</sup> (**Figure S1, Supporting Information**), the characteristic peaks agree well with those previously reported and have

been clearly broadened due to the formation of nanosized crystals.<sup>39</sup>

The XRD patterns of the **Platform 1** with the peaks at  $2\theta = 10.5^\circ, 12.8^\circ, 14.8^\circ, 16.6^\circ$ , and  $18.0^\circ$  matched the crystal planes of (022), (112), (022), (013), and (222) of the ZIF-8 nanocrystals.<sup>39</sup> (see **Figure S2, Supporting Information**).

The ZIF-8 is one of the well-known MOFs with a sodalite-like structure (**Figure 1a**). **Figure 1b** shows the TEM images of

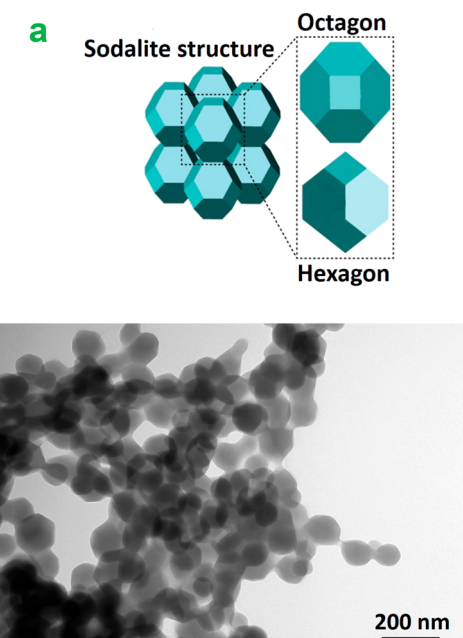


**Figure 1.** (a) Illustration of sodalite-like structure of ZIF-8 crystals and single ZIF-8 crystal. (b) TEM images of the as-synthesized ZIF-8 samples.

the as-synthesized MOF nanocrystals for characterization. Based on a view from a different angle, a single crystal with hexagonal or octagonal facet was observed. The TEM images in **Figure 1b** revealed the as-synthesized ZIF-8 nanocrystals. By using the ImageJ software program, size distribution of the ZIF-8 nanocrystals measured from the TEM photograph ranged 56.0–122.6 nm (**Figure S3 in Supporting Information**). The mean nanocrystal size was 87.4 nm, which is in accordance with that in the published work.<sup>39</sup>

To evaluate the retained amount of ZIF-8 nanocrystals on the fabrics after the hybrid fabrication, we calculated deposition ratio using the following equation:<sup>30</sup>

$$\text{deposition - ratio}(\text{wt}\%) = 100\% \times (m_2 - m_1)/m_2 \quad (1)$$

where  $m_1$  and  $m_2$  are the weights of the pristine fabric fibers without treatment and the fibers treated with ZIF-8 nanoparticles. The deposition ratio of **Platform 1** and **Platform 3** is shown in **Table 1**.

To confirm the morphology of fabricated fabric platform and compare the deposition of the ZIF-8 nanocrystals in different platforms, SEM was utilized for the illustration from various magnifications ranging maximum to 100 $\times$  (**Figure 2**).

The cotton fibers without treatment showed uniform matrixes with 10–12 µm in width. The surface of the cotton fabric was smooth before the hybrid reaction with ZIF-8 (**Figure 2a**). After the reaction, a deposition ratio of 5.0 wt %

**Table 1. Deposition Ratio of ZIF-8 Nanoparticles in Different Material Systems: Cotton Fabric Platform Treated with ZIF-8 Nanoparticles (Platform 1); Polyethylene Terephthalate Gauze Platform Treated with ZIF-8 (Platform 2); Carboxymethylated Cotton Fabric Platform Treated with ZIF-8 (Platform 3)**

	deposition ratio (wt %)
Platform 1	5
Platform 2	—
Platform 3	25

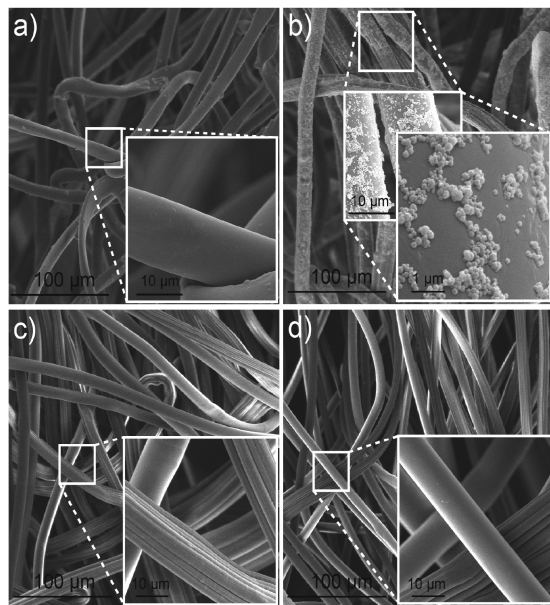


**Figure 2.** SEM images: (a) cotton fabric fibers without treatment, (b) cotton fabric fibers treated with ZIF-8 nanoparticles, (c) pure polyethylene terephthalate fabric fibers, and (d) polyethylene terephthalate fabric fibers treated with ZIF-8 nanoparticles.

(Table 1) of the ZIF-8 nanocrystals to cotton fabrics in **Platform 1** was calculated based on eq 1.

Meanwhile, the ZIF-8 nanocrystals were attached to the surface of fibers (Figure 2b). Correspondingly, polyethylene terephthalate fabric fibers were uniform with  $9\text{--}11\ \mu\text{m}$  in width (Figure 2c). However, Figure 2d revealed that the surface of the polyethylene terephthalate fabric remained neat during the hybrid reaction process, which indicated that the ZIF-8 nanocrystals failed to attach on the surface of the polyethylene terephthalate fibers.

**3.2. XPS and FTIR Analyses.** XPS was employed to investigate the evidence of chemical compositions on the sample surfaces. The XPS survey (Figure 3a and b) and an individual high-resolution element analysis were conducted for **Platform 1** (Figure 3c–f). Figure 3a shows the XPS spectra of pure cotton fabric and **Platform 1**.

For pure cotton fabric fibers, the fibers only consist of carbohydrate with two major peaks of C 1s and O 1s in the upper spectrum.

For **Platform 1**, binding energy peaks corresponding to C 1s, O 1s, N 1s, and Zn 2p were detected in Figure 3a. As illustrated in Figure 3c, characteristic peaks of Zn 2p<sub>1/2</sub> and Zn 2p<sub>3/2</sub> with the binding energy of 1044.6 and 1021.6 eV were observed. In addition, the binding energy of N 1s is at 399.4 eV (Figure 3d). The N 1s and Zn 2p peaks indicated that nitrogen

and zinc were induced after the hybrid process of **Platform 1** with an element ratio of nitrogen to zinc as 24.01% to 5.79% (Table 2).

The ratio nearly equals to 4:1, which corresponds to the content of nitrogen and zinc in the empirical chemical formula of the ZIF-8 ( $\text{C}_8\text{H}_{10}\text{N}_4\text{Zn}$ ).<sup>40</sup>

Two deconvolved peaks of N 1s were identified at 400.0 and 398.7 eV. The peak at 400.0 eV is related to the N of 2-methylimidazole ligand.<sup>41,42</sup> The peak at 398.7 eV is corresponding to oxynitride (Zn–N).<sup>43</sup> The C 1s peak at 284.9 eV can be deconvolved into three subpeaks (Figure 3e). The peak at 286.1 eV is attributed to the C–O bond, derived from glucose units in cotton, whereas the peak at 285.0 eV reveals the presence of C–N bond in MeIM-units of the ZIF-8.<sup>44</sup>

The XPS spectrum of O 1s could be fitted by the peaks at 532.0 and 530.4 eV (Figure 3f). In the cross-linked structure of the cotton fabric based on glucose units, oxygen atoms are linking to carbon atoms, partially forming hydrogen bonds.<sup>45</sup> The peak at 532.0 eV is considered to the contributions of C–O–H and C–O–H···O.<sup>45</sup> The lower binding component at 530.4 eV can be assigned to Zn–O,<sup>46,47</sup> which is the evidence of Zn–O coordination for the ZIF-8 nanocrystal attachment on the cotton fabric via chelation.

The XPS data indicate that the ZIF-8 nanocrystals were attached to the cotton fibers with an intact chemical constitution after the composite hybridization. In addition, it should be noted that the content of oxygen decreased in the composite, which is lower than the pure fabric. It is owing to a much lower percentage of oxygen in the ZIF-8 than fibers. Yet, the content of carbon changed slightly because of similar proportions of carbon in the ZIF-8 and cotton fibers. In contrast, polyethylene terephthalate fabric and **Platform 2** both only exhibit predominant narrow peaks of C 1s at 284.8 eV and O 1s at 530.1 eV. **Platform 2** did not reveal obvious elemental induction of zinc and nitrogen from the ZIF-8. These results are in quantitative agreement with the captured SEM images, which show that the ZIF-8 nanocrystals failed to be adsorbed on the polyethylene terephthalate fiber surface.

To identify and characterize the presence of functional groups in the fabrics, FTIR-ATR experiments were carried out. FTIR spectra of cotton fabric fibers, **Platform 1**, polyethylene terephthalate fibers, and **Platform 2** were shown in Figure 4. In the spectra of cotton fabric, –OH stretching and blending vibrations were observed at  $3330\ \text{cm}^{-1}$  and  $1630\ \text{cm}^{-1}$ .<sup>30</sup>

Absorption bands at 2900 and  $1370\ \text{cm}^{-1}$  revealed stretching and deformational vibrations of the C–H group in the glucose unit.<sup>48</sup> The peak at  $895\ \text{cm}^{-1}$  corresponds to the characteristic band of glycosidic linkages among glucose units.<sup>48</sup> It indicates that the original cotton fabric we used was composed of cellulose fibers.<sup>30,48</sup> Compared to the pristine cotton fabric, an increase in the signal intensity at  $1570\ \text{cm}^{-1}$  was detected in **Platform 1**. This is attributed to large amount of C=N stretch induced by the ZIF-8 nanocrystals adsorbed on the fiber surface.<sup>49</sup> Out-of-plane benzene groups were monitored at 722 and  $870\ \text{cm}^{-1}$ .<sup>30</sup>

Two absorption bands at 1410 and  $1340\ \text{cm}^{-1}$  were assigned to CH<sub>2</sub> wagging.<sup>50</sup> The broad bands at 1090 and  $1240\ \text{cm}^{-1}$  were attributed to ester C=O stretching;<sup>50</sup> meanwhile, a characteristic C=O stretching of ester appeared at  $1710\ \text{cm}^{-1}$ .<sup>37,51</sup>

The change in FTIR spectra (pink and blue curves in Figure 4) indicates that **Platform 2** was composed by complete

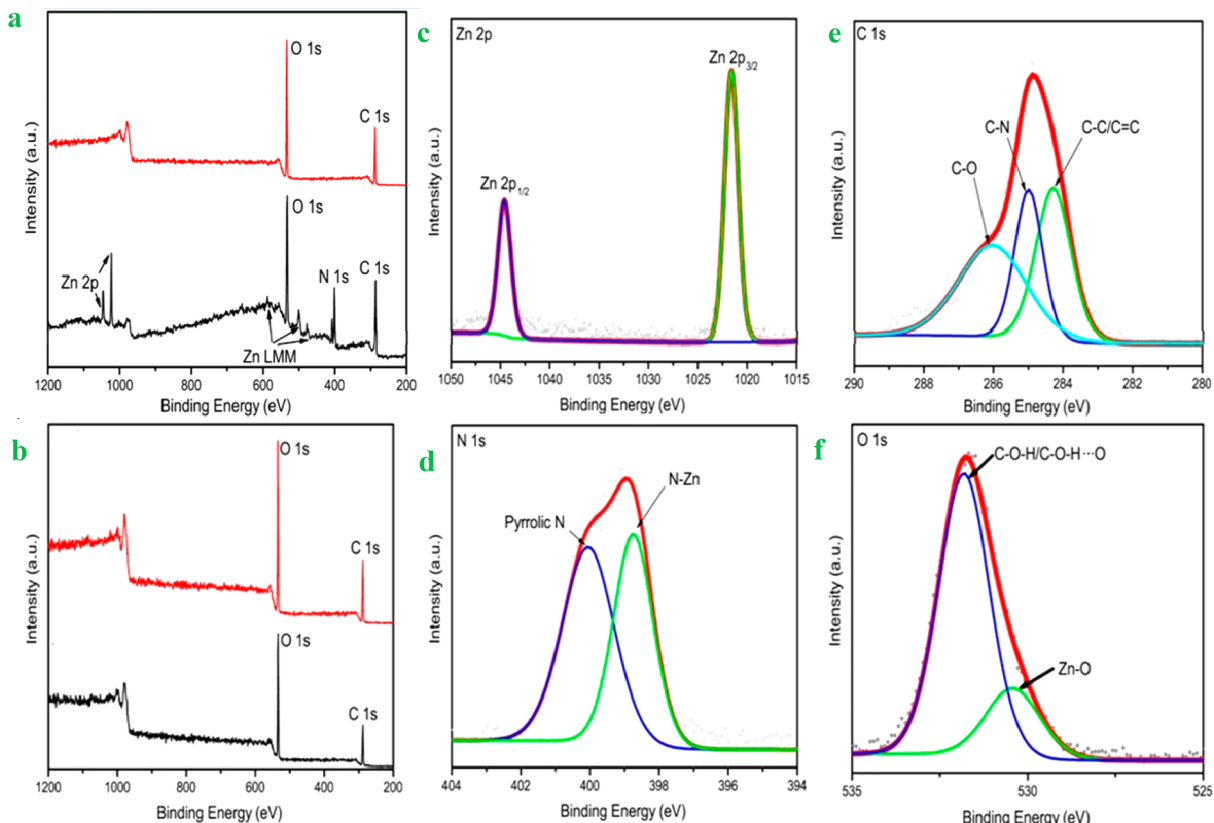


**Figure 3.** (a) XPS survey spectra of cotton fabric fiber (red line) and cotton fabric fibers treated with ZIF-8 (black line). (b) XPS survey spectra of polyethylene terephthalate fabric fibers (red line) and polyethylene terephthalate fabric fibers treated with ZIF-8 (black line). High-resolution XPS scans of (c) Zn 2p, (d) N 1s, and (f) C 1s of cotton fabric fibers treated with ZIF-8 nanoparticles.

**Table 2. Elemental Compositions of Different Fabrics and ZIF-8/Fabric Material Systems**

	cotton fabric		cotton fabric platform treated with ZIF-8 nanoparticles		polyethylene terephthalate gauze		polyethylene terephthalate gauze platform treated with ZIF-8 nanoparticles	
Elemental composition (%)	C 1s	57.5	C 1s	46.35	C 1s	47.4	C 1s	45.4
	O 1s	42.5	O 1s	31.14	O 1s	52.6	O 1s	54.6
			N 1s	18.81				
			Zn 2p	3.70				

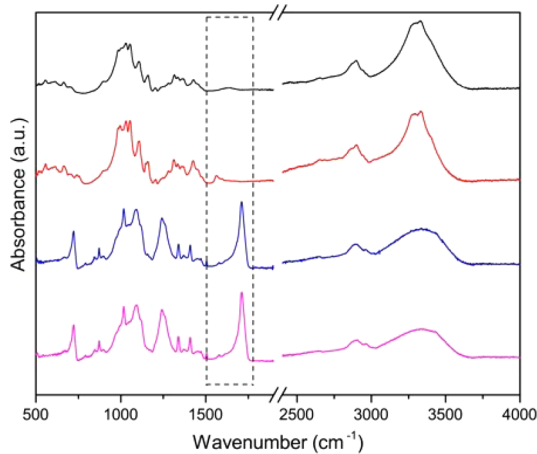


**Figure 4.** FTIR spectra of cotton fabric fibers (black curve), cotton fabric fibers treated with ZIF-8 (**Platform 1**) (red curve), polyethylene terephthalate fabric fibers (blue curve), and polyethylene terephthalate gauze platform treated with ZIF-8 (**Platform 2**) (pink curve).

polyethylene terephthalate fibers without any attachment of the ZIF-8 nanocrystals. The analyses from XPS and FTIR are in good agreement, which provided indirect evidence of the favorable attachment of the ZIF-8 nanocrystals to the cotton fabric surface rather than polyethylene terephthalate-based noncellulosic substrate. This is in good accordance with the direct evidence observed by SEM.

Key finding in this section may be outlined as follows: cotton fabrics with abundant hydroxyl groups in glucose units can interact with metal ions in MOFs,<sup>21,37,50,51</sup> leading to the attachment of the ZIF-8 nanocrystals on cotton surface via chelation of zinc (Zn–O coordination). However, polyethylene terephthalate fabrics that mainly contain carbonyl groups lack polar groups, resulting in the presence of a low surface free energy and poor wettability.<sup>52</sup> Therefore, it is hard to form interactions with the ZIF-8 nanocrystals.

### 3.3. Protein Immobilization and Enzyme Catalysis

**Assessment.** Fluorometry experiment (Figure 5a) of Alexa Fluor 647-labeled donkey anti-rabbit IgG as a fluorescent antibody was done. It was used to determine protein immobilization performance.

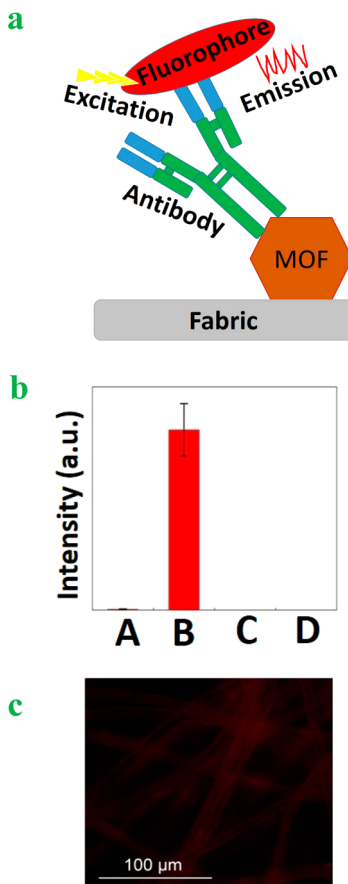


**Figure 5.** (a) Schematic of fluorometry detection of the fluorophore-labeled antibody adsorbed by ZIF-8 nanoparticles for protein immobilization on the fabric substrate. (b) Fluorescence intensity of the fabrics after being immersed in Alexa Fluor 647-labeled donkey anti-rabbit IgG solution (100  $\mu$ g/mL). Here, A: Cotton fabric; B: cotton fabric fibers treated with ZIF-8 (**Platform 1**); C: polyethylene terephthalate fabric fibers; D: polyethylene terephthalate gauze platform treated with ZIF-8 (**Platform 2**). (c) Fluorescent images (20 $\times$  objective) of the **Platform 1** with adsorption of Alexa Fluor 647-labeled donkey anti-rabbit IgG.

After being immersed in the aqueous solution in the presence of Alexa Fluor 647-labeled antibodies, **Platform 1** shows significantly higher fluorescence intensity than other fabric samples (Figure 5b and c). It supports that a great number of the ZIF-8 nanocrystals on the surface of cotton fabric was performed as grafted binding sites for protein immobilization. The results cast new light on the illustration of enhanced antibody adsorption capability through MOF-attached cotton fabric substrate. This capability is attainable due to the chelation between zinc ions on the ZIF-8 nanocrystals and histidine residues in the proteins.<sup>32</sup>

We also evaluated the biocompatibility of the fabrics based on the investigation of an enzyme-catalyzed colorimetric reaction on the MOF/fabric systems (Figure 6a). The reactions were based on the catalysis of HRP enzyme for conversion of chromogenic TMB substrates (colorless) into colored products (blue), followed by adding sulfuric acid to stabilize the color development (yellow).

As shown in Figure 6b, **Platform 1** performed a prominent signal improvement for TMB conversion reaction in the presence of HRP enzyme. Since physical interactions (e.g., van der Waals forces and electrostatic interactions) between the

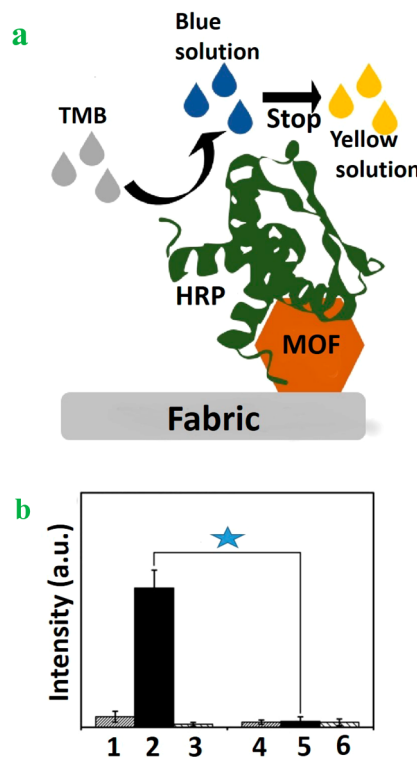


**Figure 6.** (a) Illustration of colorimetric assay of HRP enzyme immobilized by MOF nanoparticles on fabric substrate. (b) TMB coloration reaction results on pure fabrics and MOF/fabric composites ( $n = 9$ ) (\* $p$ -value < 0.001. 1, cotton fabric modified with HRP and TMB; 2, MOF/cotton fabric composites modified with HRP and TMB; 3, MOF/cotton fabric composites modified with TMB; 4, Polyethylene terephthalate fabric modified with HRP and TMB; 5, MOF/Polyethylene terephthalate fabric composites modified with HRP and TMB; 6, MOF/Polyethylene terephthalate fabric composites modified with TMB).

HRP-labeled antibodies and either cotton or polyethylene terephthalate fabrics existed,<sup>6</sup> this may cause adsorption of HRP-labeled antibodies to the ZIF-8 nanocrystals which were attached to fabric surface. Thus, weak colorimetric signals were also observed in Figure 6. However, significant adsorption of HRP-labeled antibodies on **Platform 1** appears, due to much stronger coordination between the zinc cations on the ZIF-8 nanocrystals and the carbonyl group of the enzymes.<sup>53</sup> It provides a higher signal on the TMB conversion reaction.

Moreover, the adsorption of HRP-labeled antibodies to the composite successfully maintained the bioactivity of HRP enzymes without destroying catalytic sites for realizing TMB coloration. By comparing the results of HRP catalysis on **Platform 1** in Figure 6b, it can be seen that **Platform 2** did not obviously show signal enhancement. It is in accordance with characterizations and analyses in previous discussions about the unsuccessful deposition of the ZIF-8 nanocrystals.

We also carried out control experiment for the TMB conversion reaction on **Platform 1** and **Platform 2** while the HRP-labeled antibodies are not presented (Figure 6b). There was no signal increase. It eliminated a potential suspicion of the false signal induced by MOF catalysis to TMB coloration reaction. The results proved that the higher amount of adsorbed active HRP-labeled antibodies enzymes was positively correlated with the deposition ratio of the ZIF-8

nanocrystals on cotton fabric without destroying the catalytic performance of the enzyme.

**3.4. Carboxymethylation of Cotton Fabric.** Previous studies show that the existing of hydroxyl groups in cotton fabrics makes it possible to modify cotton substrate for enhancing target immobilization.<sup>33,34</sup> In this section, we will discuss how carboxymethylation can improve the protein immobilization on cotton fabric.

As shown in Scheme 1, the metal ions in MOF can be anchored to the functional groups on the modified cellulosic substrate after a carboxymethylation process.<sup>35</sup> The carboxymethylated cotton substrate enables more active sites on cotton fabric, which can adsorb the MOF nanocrystals and thus introduce a high loading amount of the MOF through chelation and electrostatic interaction.<sup>31</sup> Comparing to pristine cotton fabric, the FTIR spectra of carboxymethylated cotton fabric show an additional absorption peak at  $1605\text{ cm}^{-1}$  and the enhanced absorption at  $1428\text{ cm}^{-1}$  (Figure 7). This

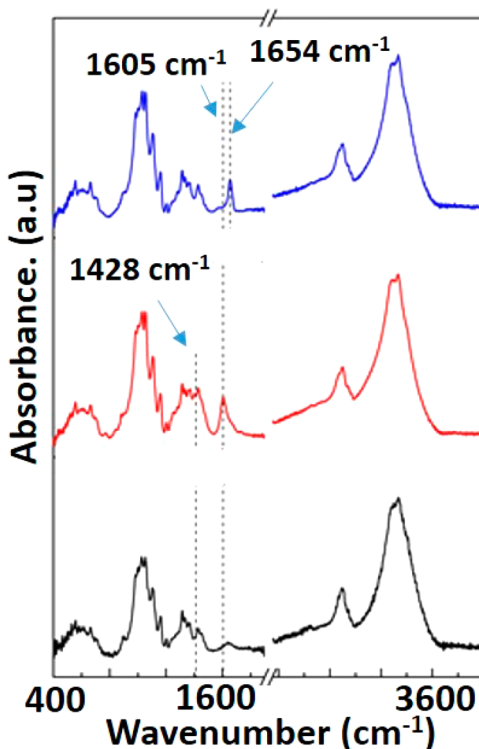


**Figure 7.** FTIR spectra of cotton fabric (black curve), carboxymethylated cotton fabric (red curve), and carboxymethylated fabric platform treated with ZIF-8 (**Platform 3**) (blue curve).

indicated the presence of carboxymethyl groups<sup>54</sup> and achieved carboxymethylation on the fabric. After the treatment of ZIF-8 nanocrystals on the carboxymethylated cotton fabric, the zinc cations in ZIF-8 form direct interactions with the carboxymethyl groups on the modified cotton fabric surface. This is may be the reason why a carbonyl signal shifted from the carboxymethylated cotton fabric at  $1605\text{ cm}^{-1}$  to Platform 3 at  $1654\text{ cm}^{-1}$ .<sup>55</sup>

Figure 8a is the SEM image of the carboxymethylated cotton fabric platform. Figure 8b,c compare the loading amount of ZIF-8 nanocrystals on the surface of pure cotton fabric and carboxymethylated cotton fabric. Clearly, direct evidence of a higher loading performance of the ZIF-8 nanocrystals on the carboxymethylated cotton fabric than that on the pure cotton

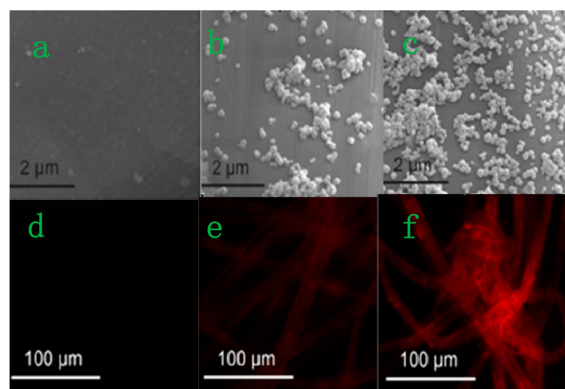


**Figure 8.** SEM images of different material systems: (a) carboxymethylated cotton fabric platform; (b) cotton fabric platform treated with ZIF-8 nanoparticles (**Platform 1**); (c) carboxymethylated cotton fabric platform treated with ZIF-8 (**Platform 3**). Fluorescent images of different material systems: (d) carboxymethylated cotton fabric platform; (e) **Platform 1**; (f) **Platform 3**.

fabric was observed. Thus, more ZIF-8 nanocrystals were attached on the surface of the modified cotton fabric with carboxymethyl groups as functionally active sites. The result may be attributed to the interaction between carboxymethyl groups on the carboxymethylated cotton fabric and zinc cations and double carbon bonds in 2-methylimidazole of the ZIF-8.<sup>55,56</sup> This is consistent with what has been found in the calculations of deposition ratio (Table 1) and FTIR data (Figure 7).

As expected, the **Platform 3** was observed to show higher fluorescence intensity than the **Platform 1**. It indicates that the **Platform 3** performed a more robust capability to immobilize Alexa Fluor 647-labeled antibodies than the **Platform 1** due to carboxymethylation (Figure 9). To eliminate a concern that

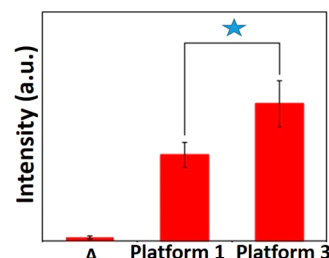


**Figure 9.** Fluorescence intensity of the Alexa Fluor 647-labeled donkey anti-rabbit IgG adsorbed on (a) carboxymethylated cotton fabric platform (represented by A in the figure); (b) cotton fabric platform treated with ZIF-8 nanoparticles (**Platform 1**); (c) carboxymethylated fabric platform treated with ZIF-8 (**Platform 3**). (\* $p$ -value < 0.05.)

carboxymethyl groups in the fibers of the **Platform 3** may improve the adsorption performance for proteins rather than the greater loadings of the ZIF-8 nanocrystals as the grafted binding sites,<sup>58</sup> another control experiment was performed using the carboxymethylated cotton fabric as the substrate.

By comparing the SEM images in Figure 2a and Figure 8a, no significant change of cotton surface morphology was captured. As shown in Figure 8d and Figure 9, carboxymethylated cotton fabric did not show obvious improvements on the adsorption of Alexa Fluor 647-labeled antibodies. Although the carboxymethylated cotton fabric has been observed with

enhanced protein adsorption behaviors,<sup>57</sup> the environmental pH value (7.4 in PBS buffer) restricted the protein adsorption on the carboxymethylated cotton fabric in the case of our work. Here, enhanced protein immobilizations on **Platform 3** is considered due to the increased loadings of the ZIF-8 nanocrystals compared to **Platform 1**. It implies that the carboxymethylation process on cotton fabric boosts the ability to MOF nanocrystal attachment and then protein immobilization. It is possible that with higher uptake of the ZIF-8 nanocrystals, more ion-exchange sites are contained in the material systems and more adsorbent–adsorbate interactions are associated with  $\pi$ – $\pi$  stacking.<sup>58,59</sup>

The method introduced in this article may provide a versatile strategy for enhancement of protein immobilization when considering the existing of huge number of MOFs classes.

ZIF-8 is shown to be eventually and densely distributed on the surface of  $\text{SiO}_2$ <sup>60</sup> and polyacrylonitrile nanofibers<sup>61</sup> as well as wool fabric.<sup>62</sup> The composites made are reported to show synergistic promoting effect on particulate matter capture and gas pollutant adsorption,<sup>60</sup> as well as the ability of removing tetracycline<sup>61</sup> and pharmaceutical intermediate from wastewater.<sup>62</sup> Their investigations imply that ZIF-8 based composites are flexible platforms for matter adsorption. They are envisioned to be used in industry in terms of their huge potential.

Our study has not provided detailed investigation of mechanical stability of these MOF/fabric substrates. For instance, how will these MOF/fabric substrates perform after bending for tens of times? The future study of these would help us to design more robust substrates for the protein immobilization. Nevertheless, our investigation has established a possible method for enhanced protein adsorption in fibrous substrates through treatment with ZIF-8 nanoparticles.

In future application, we can expect the origami of the MOFs modified cotton fabric substrates to provide a three-dimensional platform for the protein immobilization and bioanalysis. These platforms combined with microfluidics can become a new class of point-of-care diagnostic devices, which are envisioned to hold similar functions as those microfluidic paper-based analytical devices ( $\mu\text{PAD}$ ).<sup>63,64</sup> Future endeavor may be focused on the study of protein adsorption capacity, protein adsorption stability, kinetic process in the protein adsorption, quantitative analysis of proteins, and the relation between metal content and adsorption capacity, which leads to a much deeper understanding of these platforms.<sup>65–77</sup>

## 4. CONCLUSIONS

This work presents a useful method for fabricating of MOF/fabric substrates with the ability of protein adsorption. The MOF/cotton fabric (**Platform 1**) is demonstrated with 5.0 wt % loading of uniformly distributed the ZIF-8 nanocrystals on fabric surface, and an increased 25 wt % loading on carboxymethylated cotton fabric. Unlike the cotton fabric, polyethylene terephthalate fabric does not reveal a MOF loading phenomenon. Due to the ZIF-8 nanocrystal attachments, the cotton surface has enabled more grafted binding sites for protein adsorption, promising for biomolecule immobilization. The MOF/cotton fabric not only reveals an enhanced capability of protein adsorption, but also provides favorable biocompatibility to maintain the bioactivity of enzymes. We also evaluated the protein adsorption of the carboxymethylated cotton fabric platform treated with the ZIF-

8 (**Platform 3**); it showed better ability to immobilize the Alexa Fluor 647-labeled antibodies than **Platform 1** due to the carboxymethylation. These novel material systems will potentially be used in making biomolecule carriers, flexible sensing devices, and fillers. The making of these new substrates for protein immobilization through simple chemistry will be envisioned to raise the interest of the biochemical industry.

## ■ ASSOCIATED CONTENT

### S Supporting Information

The Supporting Information is available free of charge at <https://pubs.acs.org/doi/10.1021/acsanm.9b01717>.

Simulated and experimental XRD patterns for ZIF-8 nanocrystals (Figure S1). XRD profile of ZIF-8 and cotton fabric platform treated with ZIF-8 (Figure S2). (PDF)

## ■ AUTHOR INFORMATION

### Corresponding Authors

\*E-mail: pengfei.song@xjtu.edu.cn.

\*E-mail: yangjiquan@njnu.edu.cn.

\*E-mail: chemwuye@njnu.edu.cn.

### ORCID

Pengfei Ou: 0000-0002-3630-0385

Ye Wu: 0000-0002-4831-9729

### Author Contributions

<sup>†</sup>H.F. and P.O. contributed equally.

### Notes

The authors declare no competing financial interest.

## ■ ACKNOWLEDGMENTS

The authors appreciate the financial support from China National Key R&D Program (2017YFB1103202), Jiangsu State R&D Program (BE2018010), Key Program Special Fund in XJTLU (KSF-E-39), XJTLU Research Development Fund (RDF-18-02-20). Special thanks to Dr. Xiaochu Wu (TEM), Dr. Lea Gustin (XRD), and Lin Song (FTIR and XPS) for offering help and valuable discussions.

## ■ REFERENCES

- (1) Nakanishi, K.; Sakiyama, T.; Imamura, K. On the adsorption of proteins on solid surfaces, a common but very complicated phenomenon. *J. biosci. bioeng.* **2001**, *91*, 233–244.
- (2) Rabe, M.; Verdes, D.; Seeger, S. Understanding protein adsorption phenomena at solid surfaces. *Adv. Colloid Interface Sci.* **2011**, *162*, 87–106.
- (3) Absolom, D.; Zingg, W.; Neumann, A. Protein adsorption to polymer particles: role of surface properties. *J. Biomed. Mater. Res.* **1987**, *21*, 161–171.
- (4) Bernard, A.; Renault, J. P.; Michel, B.; Bosshard, H. R.; Delamarche, E. Microcontact printing of proteins. *Adv. Mater.* **2000**, *12*, 1067–1070.
- (5) Souzandeh, H.; Johnson, K. S.; Wang, Y.; Bhamidipaty, K.; Zhong, W.-H. Soy-protein-based nanofabrics for highly efficient and multifunctional air filtration. *ACS Appl. Mater. Interfaces* **2016**, *8*, 20023–20031.
- (6) Pelton, R. Bioactive paper provides a low-cost platform for diagnostics. *TrAC, Trends Anal. Chem.* **2009**, *28*, 925–942.
- (7) Grafarend, D.; Calvet, J. L.; Klinkhammer, K.; Salber, J.; Dalton, P. D.; Möller, M.; Klee, D. Control of protein adsorption on functionalized electrospun fibers. *Biotechnol. Bioeng.* **2008**, *101*, 609–621.

- (8) Gusakov, A. V.; Sinitsyn, A. P.; Markov, A. V.; Sinitsyna, O. A.; Ankudimova, N. V.; Berlin, A. G. Study of protein adsorption on indigo particles confirms the existence of enzyme–indigo interaction sites in cellulase molecules. *J. Biotechnol.* **2001**, *87*, 83–90.
- (9) Kim, M.; Sasaki, M.; Saito, K.; Sugita, K.; Sugo, T. Protein Adsorption Characteristics of a Sulfonic-Acid-Group-Containing Nonwoven Fabric. *Biotechnol. prog.* **1998**, *14*, 661–663.
- (10) Woo, K. M.; Chen, V. J.; Ma, P. X. Nano-fibrous scaffolding architecture selectively enhances protein adsorption contributing to cell attachment. *J. Biomed. Mater. Res.* **2003**, *67*, 531–537.
- (11) Jones, K. L.; O’Melia, C. R. Protein and humic acid adsorption onto hydrophilic membrane surfaces: effects of pH and ionic strength. *J. Membr. Sci.* **2000**, *165*, 31–46.
- (12) Beltrame, P. L.; Carniti, P.; Focher, B.; Marzetti, A.; Cattaneo, M. Cotton Cellulose - Enzyme Adsorption and Enzymatic-Hydrolysis. *J. Appl. Polym. Sci.* **1982**, *27*, 3493–3502.
- (13) Jarujamrus, P.; Tian, J.; Li, X.; Siripinyanond, A.; Shiowatana, J.; Shen, W. Mechanisms of red blood cells agglutination in antibody-treated paper. *Analyst* **2012**, *137*, 2205–2210.
- (14) Lu, G.; Hupp, J. T. Metal– organic frameworks as sensors: a ZIF-8 based Fabry–Pérot device as a selective sensor for chemical vapors and gases. *J. Am. Chem. Soc.* **2010**, *132*, 7832–7833.
- (15) Lu, X.; Wang, X.; Wu, L.; Wu, L.; Fu, L.; Gao, Y.; Chen, J. Response Characteristics of Bisphenols on a Metal–Organic Framework-Based Tyrosinase Nanosensor. *ACS Appl. Mater. Interfaces* **2016**, *8*, 16533–16539.
- (16) Lu, X.; Ye, J.; Zhang, D.; Xie, R.; Bogale, R. F.; Sun, Y.; Zhao, L.; Zhao, Q.; Ning, Q. Silver carboxylate metal–organic frameworks with highly antibacterial activity and biocompatibility. *J. Inorg. Biochem.* **2014**, *138*, 114–121.
- (17) Abdelhameed, R. M.; Abdel-Gawad, H.; Elshahat, M.; Emam, H. E. Cu–BTC@ cotton composite: design and removal of ethion insecticide from water. *RSC Adv.* **2016**, *6*, 42324–42333.
- (18) Wang, C.; Qian, X.; An, X. In situ green preparation and antibacterial activity of copper-based metal–organic frameworks/ cellulose fibers (HKUST-1/CF) composite. *Cellulose* **2015**, *22*, 3789–3797.
- (19) Hamed, M. M.; Hajian, A.; Fall, A. B.; Håkansson, K.; Salajkova, M.; Lundell, F.; Wågberg, L.; Berglund, L. A. Highly conducting, strong nanocomposites based on nanocellulose-assisted aqueous dispersions of single-wall carbon nanotubes. *ACS Nano* **2014**, *8*, 2467–2476.
- (20) Achmann, S.; Hagen, G.; Kita, J.; Malkowsky, I. M.; Kiener, C.; Moos, R. Metal–organic frameworks for sensing applications in the gas phase. *Sensors* **2009**, *9*, 1574–1589.
- (21) Küsgens, P.; Siegle, S.; Kaskel, S. Crystal Growth of the Metal–Organic Framework  $\text{Cu}_3(\text{BTC})_2$  on the Surface of Pulp Fibers. *Adv. Eng. Mater.* **2009**, *11*, 93–95.
- (22) Li, Z.; Yang, L.; Cao, H.; Chang, Y.; Tang, K.; Cao, Z.; Chang, J.; Cao, Y.; Wang, W.; Gao, M.; Liu, C.; Liu, D.; Zhao, H.; Zhang, Y.; Li, M. Carbon materials derived from chitosan/cellulose cryogel-supported zeolite imidazole frameworks for potential supercapacitor application. *Carbohydr. Polym.* **2017**, *175*, 223–230.
- (23) Jung, S.; Kim, Y.; Kim, S.-J.; Kwon, T.-H.; Huh, S.; Park, S. Bio-functionalization of metal–organic frameworks by covalent protein conjugation. *Chem. Commun.* **2011**, *47*, 2904–2906.
- (24) Deng, H.; Grunder, S.; Cordova, K. E.; Valente, C.; Furukawa, H.; Hmadeh, M.; Gándara, F.; Whalley, A. C.; Liu, Z.; Asahina, S.; Kazumori, H.; O’Keeffe, M.; Terasaki, O.; Stoddart, J. F.; Yaghi, O. M. Large-pore apertures in a series of metal–organic frameworks. *Science* **2012**, *336*, 1018–1023.
- (25) Liang, K.; Carbonell, C.; Styles, M. J.; Ricco, R.; Cui, J.; Richardson, J. J.; Maspoch, D.; Caruso, F.; Falcaro, P. Biomimetic replication of microscopic metal–organic framework patterns using printed protein patterns. *Adv. Mater.* **2015**, *27*, 7293–7298.
- (26) Park, K. S.; Ni, Z.; Côté, A. P.; Choi, J. Y.; Huang, R.; Uribe-Romo, F. J.; Chae, H. K.; O’Keeffe, M.; Yaghi, O. M. Exceptional chemical and thermal stability of zeolitic imidazolate frameworks. *Proc. Natl. Acad. Sci. U. S. A.* **2006**, *103*, 10186–10191.
- (27) Liang, K.; Ricco, R.; Doherty, C. M.; Styles, M. J.; Bell, S.; Kirby, N.; Mudie, S.; Haylock, D.; Hill, A. J.; Doonan, C. J.; Falcaro, P. Biomimetic mineralization of metal–organic frameworks as protective coatings for biomacromolecules. *Nat. Commun.* **2015**, *6*, 7240.
- (28) Ghosh, P. *Colloid and interface science*; PHI Learning Pvt. Ltd., 2009.
- (29) Liang, K.; Wang, R.; Boutter, M.; Doherty, C. M.; Mulet, X.; Richardson, J. J. Biomimetic mineralization of metal–organic frameworks around polysaccharides. *Chem. Commun.* **2017**, *53*, 1249–1252.
- (30) Su, Z.; Zhang, M.; Lu, Z.; Song, S.; Zhao, Y.; Hao, Y. Functionalization of cellulose fiber by in situ growth of zeolitic imidazolate framework-8 (ZIF-8) nanocrystals for preparing a cellulose-based air filter with gas adsorption ability. *Cellulose* **2018**, *25*, 1997–2008.
- (31) Kyzas, G. Z.; Siafaka, P. I.; Pavlidou, E. G.; Chrissafis, K. J.; Bikaris, D. N. Synthesis and adsorption application of succinyl-grafted chitosan for the simultaneous removal of zinc and cationic dye from binary hazardous mixtures. *Chem. Eng. J.* **2015**, *259*, 438–448.
- (32) Zheng, J.; Lin, Z.; Lin, G.; Yang, H.; Zhang, L. Preparation of magnetic metal–organic framework nanocomposites for highly specific separation of histidine-rich proteins. *J. Mater. Chem. B* **2015**, *3*, 2185–2191.
- (33) da Silva Pinto, M.; Sierra-Avila, C. A.; Hinestroza, J. P. In situ synthesis of a Cu-BTC metal–organic framework (MOF 199) onto cellulosic fibrous substrates: cotton. *Cellulose* **2012**, *19*, 1771–1779.
- (34) Habibi, Y.; Lucia, L. A.; Rojas, O. J. Cellulose nanocrystals: chemistry, self-assembly, and applications. *Chem. Rev.* **2010**, *110*, 3479–3500.
- (35) Laurila, E.; Thunberg, J.; Argent, S. P.; Champness, N. R.; Zacharias, S.; Westman, G.; Ohrström, L. Enhanced Synthesis of Metal–Organic Frameworks on the Surface of Electrospun Cellulose Nanofibers. *Adv. Eng. Mater.* **2015**, *17*, 1282–1286.
- (36) Ng, R.; Zhang, X.; Liu, N.; Yang, S.-T. Modifications of nonwoven polyethylene terephthalate fibrous matrices via NaOH hydrolysis: Effects on pore size, fiber diameter, cell seeding and proliferation. *Process Biochem.* **2009**, *44*, 992–998.
- (37) Emam, H. E.; Darwesh, O. M.; Abdelhameed, R. M. In-growth metal organic framework/synthetic hybrids as antimicrobial fabrics and its toxicity. *Colloids Surf., B* **2018**, *165*, 219–228.
- (38) Bennett, T. D.; Keen, D. A.; Tan, J.-C.; Barney, E. R.; Goodwin, A. L.; Cheetham, A. K. Thermal amorphization of zeolitic imidazolate frameworks. *Angew. Chem., Int. Ed.* **2011**, *50*, 3067–3071.
- (39) Pan, Y.; Liu, Y.; Zeng, G.; Zhao, L.; Lai, Z. Rapid synthesis of zeolitic imidazolate framework-8 (ZIF-8) nanocrystals in an aqueous system. *Chem. Commun.* **2011**, *47*, 2071–2073.
- (40) Wu, H.; Zhou, W.; Yildirim, T. Hydrogen storage in a prototypical zeolitic imidazolate framework-8. *J. Am. Chem. Soc.* **2007**, *129*, 5314–5315.
- (41) Chen, Y.-M.; Liang, W.; Li, S.; Zou, F.; Bhaway, S. M.; Qiang, Z.; Gao, M.; Vogt, B. D.; Zhu, Y. A nitrogen doped carbonized metal–organic framework for high stability room temperature sodium–sulfur batteries. *J. Mater. Chem. A* **2016**, *4*, 12471–12478.
- (42) Yu, G.; Sun, J.; Muhammad, F.; Wang, P.; Zhu, G. Cobalt-based metal organic framework as precursor to achieve superior catalytic activity for aerobic epoxidation of styrene. *RSC Adv.* **2014**, *4*, 38804–38811.
- (43) Li, C.; Hu, C.; Zhao, Y.; Song, L.; Zhang, J.; Huang, R.; Qu, L. Decoration of graphene network with metal–organic frameworks for enhanced electrochemical capacitive behavior. *Carbon* **2014**, *78*, 231–242.
- (44) Attfield, M. P.; Cubillas, P. Crystal growth of nanoporous metal organic frameworks. *Dalton Trans.* **2012**, *41*, 3869–3878.
- (45) Yao, Q.; Fan, B.; Xiong, Y.; Jin, C.; Sun, Q.; Sheng, C. 3D assembly based on 2D structure of cellulose nanofibril/graphene oxide hybrid aerogel for adsorptive removal of antibiotics in water. *Sci. Rep.* **2017**, *7*, 45914.

- (46) Das, J.; Pradhan, S. K.; Sahu, D. R.; Mishra, D. K.; Sarangi, S. N.; Nayak, B. B.; Verma, S.; Roul, B. K. Micro-Raman and XPS studies of pure ZnO ceramics. *Phys. B* **2010**, *405*, 2492–2497.
- (47) Fan, F.; Tang, P.; Wang, Y.; Feng, Y.; Chen, A.; Luo, R.; Li, D. Facile synthesis and gas sensing properties of tubular hierarchical ZnO self-assembled by porous nanosheets. *Sens. Actuators, B* **2015**, *215*, 231–240.
- (48) Abderrahim, B.; Abderrahman, E.; Mohamed, A.; Fatima, T.; Abdesselam, T.; Krim, O. Kinetic thermal degradation of cellulose, polybutylene succinate and a green composite: comparative study. *World J. Envir. Eng.* **2015**, *3*, 95.
- (49) dos Santos Ferreira da Silva, J.; Lopez Malo, D.; Anceski Bataglion, G.; Nogueira Eberlin, M.; Machado Ronconi, C.; Alves Junior, S.; de Sa, G. F. Adsorption in a Fixed-Bed Column and Stability of the Antibiotic Oxytetracycline Supported on Zn (II)-[2-Methylimidazolate] Frameworks in Aqueous Media. *PLoS One* **2015**, *10*, No. e0128436.
- (50) Andanson, J. M.; Kazarian, S. G. In situ ATR-FTIR Spectroscopy of Poly (ethylene terephthalate) Subjected to High-Temperature Methanol. *Macromol. Symp.* **2008**, *265*, 195–204.
- (51) Huang, Z.; Bi, L.; Zhang, Z.; Han, Y. Effects of dimethylolpropionic acid modification on the characteristics of polyethylene terephthalate fibers. *Mol. Med. Rep.* **2012**, *6*, 709–715.
- (52) Riccardi, C.; Barni, R.; Sellì, E.; Mazzone, G.; Massafra, M. R.; Marcandalli, B.; Poletti, G. Surface modification of poly (ethylene terephthalate) fibers induced by radio frequency air plasma treatment. *Appl. Surf. Sci.* **2003**, *211*, 386–397.
- (53) Feng, Y.; Schmidt, A.; Weiss, R. Compatibilization of polymer blends by complexation. 1. spectroscopic characterization of ion–amide interactions in ionomer/polyamide blends. *Macromolecules* **1996**, *29*, 3909–3917.
- (54) Qi, H.; Liebert, T.; Meister, F.; Heinze, T. Homogenous carboxymethylation of cellulose in the NaOH/urea aqueous solution. *React. Funct. Polym.* **2009**, *69*, 779–784.
- (55) Nafisi, S.; Sadjadi, A. S.; Zadeh, S. S.; Damerchelli, M. Interaction of metal ions with caffeine and theophylline: stability and structural features. *J. Biomol. Struct. Dyn.* **2003**, *21*, 289–295.
- (56) Liédana, N.; Galve, A.; Rubio, Cs.; Téllez, C.; Coronas, J. CAF@ZIF-8: one-step encapsulation of caffeine in MOF. *ACS Appl. Mater. Interfaces* **2012**, *4*, 5016–5021.
- (57) Lin, Q.; Zheng, Y.; Wang, G.; Shi, X.; Zhang, T.; Yu, J.; Sun, J. Protein adsorption behaviors of carboxymethylated bacterial cellulose membranes. *Int. J. Biol. Macromol.* **2015**, *73*, 264–269.
- (58) Zheng, J.; Lin, Z.; Lin, G.; Yang, H.; Zhang, L. Preparation of magnetic metal–organic framework nanocomposites for highly specific separation of histidine-rich proteins. *J. Mater. Chem. B* **2015**, *3*, 2185.
- (59) Jonckheere, D.; Steele, J. A.; Claes, B.; Bueken, B.; Claes, L.; Lagrain, B.; Roeffaers, M. B. J.; De Vos, D. E. Adsorption and separation of aromatic amino acids from aqueous solutions using metal–organic frameworks. *ACS Appl. Mater. Interfaces* **2017**, *9*, 30064–30073.
- (60) Zhu, Q.; Tang, X.; Feng, S.; Zhong, Z.; Yao, J.; Yao, Z. ZIF-8@SiO<sub>2</sub> composite nanofiber membrane with bioinspired spider web-like structure for efficient air pollution control. *J. Membr. Sci.* **2019**, *581*, 252–261.
- (61) Chao, S.; Li, X.; Li, Y.; Wang, Y.; Wang, C. Preparation of polydopamine-modified zeolitic imidazolate framework-8 functionalized electrospun fibers for efficient removal of tetracycline. *J. Colloid Interface Sci.* **2019**, *552*, 506–516.
- (62) Abdelhameed, R. M.; Emam, H. E. Design of ZIF(Co & Zn)@wool composite for efficient removal of pharmaceutical intermediate from wastewater. *J. Colloid Interface Sci.* **2019**, *552*, 494–505.
- (63) Martinez, A. W.; Phillips, S. T.; Whitesides, G. M. Diagnostics for the Developing World: Microfluidic Paper-Based Analytical Devices. *Anal. Chem.* **2010**, *82*, 3–10.
- (64) Kim, D.; Herr, A. E. Protein immobilization techniques for microfluidic assays. *Biomicrofluidics* **2013**, *7*, 1–45.
- (65) Kim, Y.; Yang, T.; Yun, G.; Ghasemian, M. B.; Koo, J.; Lee, E.; Cho, S. J.; Kim, K. Hydrolytic transformation of microporous metal–organic frameworks to hierarchical micro-and mesoporous MOFs. *Angew. Chem., Int. Ed.* **2015**, *54*, 13273–13278.
- (66) Wang, X.; Makal, T. A.; Zhou, H. C. Protein immobilization in metal–organic frameworks by covalent binding. *Aust. J. Chem.* **2014**, *67*, 1629–1631.
- (67) Liu, G.; Xu, Y.; Han, Y.; Wu, J.; Xu, J.; Meng, H. Immobilization of lysozyme proteins on a hierarchical zeolitic imidazolate framework(ZIF-8). *Dalton Trans.* **2017**, *46*, 2114–2121.
- (68) Chen, Y.; Lykourinou, V.; Hoang, T.; Ming, L.-J.; Ma, S. Size-selective biocatalysis of myoglobin immobilized into a mesoporous metal–organic framework with hierarchical pore sizes[J]. *Inorg. Chem.* **2012**, *51*, 9156–9158.
- (69) Lykourinou, V.; Chen, Y.; Wang, X.-S.; Meng, L.; Hoang, T.; Ming, L.-J.; Musselman, R. L.; Ma, S. Immobilization of MP-11 into a mesoporous metal–organic framework, MP-11@ mesoMOF: a new platform for enzymatic catalysis. *J. Am. Chem. Soc.* **2011**, *133*, 10382–10385.
- (70) Jung, S.; Kim, Y.; Kim, S.-J.; Kwon, T.-H.; Huh, S.; Park, S. Biofunctionalization of metal–organic frameworks by covalent protein conjugation. *Chem. Commun.* **2011**, *47*, 2904–2906.
- (71) Li, Y.; Liu, J.; Zhang, K.; Lei, L.; Lei, Z. UiO-66-NH2@PMAA: A Hybrid Polymer–MOFs Architecture for Pectinase Immobilization. *Ind. Eng. Chem. Res.* **2018**, *57*, 559–567.
- (72) Wen, L.; Gao, A.; Cao, Y.; Svec, F.; Tan, T.; Lv, Y. Layer-by-layer assembly of metal–organic frameworks in macroporous polymer monolith and their use for enzyme immobilization. *Macromol. Rapid Commun.* **2016**, *37*, 551–557.
- (73) Ahmed, I. N.; Yang, X. L.; Dubale, A. A.; Li, R.-F.; Ma, Y.-M.; Wang, L.-M.; Hou, G.-H.; Guan, R.-F.; Xie, M.-H. Hydrolysis of cellulose using cellulase physically immobilized on highly stable zirconium based metal–organic frameworks. *Bioresour. Technol.* **2018**, *270*, 377–382.
- (74) Cao, S. L.; Yue, D. M.; Li, X. H.; Smith, T. J.; Li, N.; Zong, L.-H.; Wu, H.; Ma, Y.-Z.; Lou, W.-Y. Novel nano-/micro-biocatalyst: soybean epoxide hydrolase immobilized on UiO-66-NH2MOF for efficient biosynthesis of enantiopure (R)-1, 2-octanediol in deep eutectic solvents. *ACS Sustainable Chem. Eng.* **2016**, *4*, 3586–3595.
- (75) Zhang, C.; Wang, X.; Hou, M.; Li, X.; Wu, X.; Ge, J. Immobilization on metal–organic framework engenders high sensitivity for enzymatic electrochemical detection. *ACS Appl. Mater. Interfaces* **2017**, *9*, 13831–13836.
- (76) Garcia-Galan, C.; Berenguer-Murcia, A.; Fernandez-Lafuente, R.; Rodrigues, R. C. Potential of different enzyme immobilization strategies to improve enzyme performance. *Adv. Synth. Catal.* **2011**, *353*, 2885–2904.
- (77) Bao, T.; Tang, P.; Kong, D.; Mao, Z.; Chen, Z. Polydopamine-supported immobilization of covalent-organic framework-5 in capillary as stationary phase for electrochromatographic separation. *J. Chromatography A* **2016**, *1445*, 140–148.